

Platelets and MMP-9 contribute to esophageal cancer invasion via CD40-CD154 interactions

KAZUFUMI UMEMOTO^{1,2}, TORU NAKAMURA², KATSUNORI SASAKI²,
OSAMU SATO², TOMOHIRO SUZUKI² and SATOSHI HIRANO²

¹Department of Gastroenterological Surgery II, Graduate School of Medicine, Hokkaido University, Sapporo, Hokkaido 060-8638, Japan;

²Department of Gastroenterological Surgery II, Faculty of Medicine, Hokkaido University, Sapporo, Hokkaido 060-8638, Japan

Received October 28, 2024; Accepted March 17, 2025

DOI: 10.3892/or.2025.8912

Abstract. CD40 expression in esophageal cancer (EC) is linked to poor prognosis, although its molecular role remains unclear. The present study explored the function of CD40 in EC progression and metastasis, focusing on its interaction with CD154 and the upregulation of MMP-9. CD40 expression was confirmed in EC cell lines using quantitative PCR, western blotting, flow cytometry and immunocytochemistry. Functional assays showed that recombinant soluble CD154 stimulation enhanced the migration and invasion of CD40-overexpressing EC cells without affecting viability. Co-culture experiments with platelets demonstrated that platelet-derived CD154 acted on CD40-overexpressing esophageal cancer cells, leading to upregulation of MMP-9 secretion, potentially driving tumor invasiveness. Serum analysis of patients who underwent esophagectomy revealed that low MMP-9 levels were associated with longer survival in pathological Stage I, whereas the opposite trend was observed in stages II-IV. These findings indicated that CD40 activation enhanced tumor cell invasiveness through MMP-9 upregulation. This dual role of CD40, enhancing antitumor immunity via its expression on antigen-presenting cells, while promoting tumor invasiveness through MMP-9 secretion when expressed on esophageal cancer cells, may complicate immunotherapeutic strategies

targeting CD40, as such interventions could inadvertently promote malignancy within the tumor microenvironment.

Introduction

Esophageal cancer (EC) is the eighth most common malignant tumor worldwide (1) and the sixth leading cause of cancer-related deaths (2). The number of deaths resulting from EC has decreased due to advances in surgery, chemotherapy and radiation therapy; however, the results have been unsatisfactory (1). Therefore, elucidating the molecular mechanisms underlying EC growth and metastasis, and developing novel targeted therapies to overcome therapeutic resistance are crucial for improving treatment outcomes.

CD40 is a member of the tumor necrosis factor receptor superfamily. CD40 is primarily detected on the surface of antigen-presenting cells (APCs), such as B cells, macrophages/monocytes and dendritic cells (3,4). CD40 activation stimulates multiple signaling pathways, including the NF- κ B and PI3K signaling pathways, leading to immune responses (5,6). CD40 signaling polarizes macrophages to the M1 phenotype, exerting strong antitumor effects (7), inducing dendritic cell maturation and enhancing antigen presentation (3,4). CD40 acts as a co-stimulatory molecule when APCs present antigens to CD4⁺ T lymphocytes, serving an essential role in adaptive immunity (8). CD40 is also expressed in various malignancies, including malignant melanoma, gastric cancer and lung cancer, and its expression in cancer cells such as EC cells is associated with poor prognosis (9-15). However, to the best of our knowledge, the molecular function of CD40 expression on the surface of EC cells and why it is a poor prognostic factor remain unclear.

MMP-9 is involved in breaking down the extracellular matrix (ECM) in normal physiological processes, such as embryonic development, reproduction and tissue remodeling, as well as in disease processes, including cancer metastasis (16,17). MMP-9 serves a crucial role in cancer cell invasion, migration and angiogenesis (18-20). In non-cancer cells such as human podocytes, CD40 receptor activation induces MMP-9 secretion, which is involved in ECM degradation (21). However, to the best of our knowledge, this phenomenon has not been confirmed in cancer cells. Therefore, the present study aimed to evaluate CD40 activation-induced

Correspondence to: Dr Toru Nakamura, Department of Gastroenterological Surgery II, Faculty of Medicine, Hokkaido University, North 15, West 7, Kita-ku, Sapporo, Hokkaido 060-8638, Japan

E-mail: torunakamura@med.hokudai.ac.jp

Abbreviations: APC, antigen-presenting cell; DFS, disease-free survival; EC, esophageal cancer; ECM, extracellular matrix; ESCC, esophageal squamous cell carcinoma; LAMC2, laminin subunit γ -2; PBMC, peripheral blood mononuclear cell; PLG, plasminogen; TME, tumor microenvironment; RT-qPCR, reverse transcription-quantitative PCR; sCD154, soluble CD154; rsCD154, recombinant sCD154

Key words: EC, MMP-9, CD40, CD154, invasion

changes in cancer cell bioactivity and MMP-9 upregulation. We hypothesized that CD40 regulates MMP-9 secretion, which is crucial for EC cells to acquire malignant potential.

Materials and methods

Cell culture. TE-1, -4, -5, -6, -8, -9, -10, -11, -14 and -15 human esophageal squamous cancer cell lines were purchased from the Cell Resource Center for Biomedical Research, Institute of Development, Aging and Cancer, Tohoku University (Sendai, Japan). All cells were cultured in RPMI-1640 medium (Thermo Fisher Scientific, Inc.) containing 10% (v/v) FBS (Thermo Fisher Scientific, Inc.) and 1% (v/v) penicillin-streptomycin solution (Thermo Fisher Scientific, Inc.) at 37°C in a humidified incubator with 5% CO₂. To evaluate morphological differences among these cell lines, cells at 50-70% confluency were fixed and stained using a Diff-Quick staining kit (Sysmex Corporation). The cells were sequentially immersed for 2 min each in the fixative solution, stain solution I and stain solution II at room temperature. Stained cells were observed under a BZ-9000 light microscope (Keyence Corporation) at a magnification of x20 and analyzed using the dedicated BZ-H3C software (version 1.4.1; Keyence Corporation).

Peripheral blood mononuclear cell (PBMC) isolation. Peripheral venous blood samples were collected from healthy adult donors (male; median age, 38 years; age range, 36-60 years) at Hokkaido University (Sapporo, Japan) between July 2024 and September 2024. All participants provided written informed consent prior to participation. Inclusion criteria included age ≥ 20 years and the ability to provide informed consent. Individuals with a history of cancer or active malignant disease were excluded. The present study was approved (approval no. 24-0126; approval date July 10, 2024) by the Institutional Review Board Committee of Hokkaido University (Sapporo, Japan). Blood collection from healthy donors began in July 2024, and the samples were subsequently used for experiments. PBMCs were isolated from heparinized blood samples via density gradient centrifugation at 400 x g for 30 min at room temperature using Ficoll-Paque Plus reagent (GE Healthcare) according to the manufacturer's instructions.

Western blotting. Cells were lysed using an ULTRARIPA kit (BioDynamics Laboratory, Inc.) supplemented with a Protease Inhibitor Cocktail (Promega Corporation). Protein concentrations were determined using the TaKaRa BCA Protein Assay Kit (Takara Bio Inc.). Equal amounts of protein (10 μ g per lane) were loaded onto 15% SDS-PAGE gels and transferred to PVDF membranes (Bio-Rad Laboratories, Inc.). Human PBMCs were used as positive controls. After protein transfer to the PVDF membranes, the membranes were blocked with Tris-buffered saline with 0.1% Tween-20 (TBST) and 5% skim milk at room temperature for 1 h, and then incubated with primary antibodies overnight at 4°C. A list of the antibodies used in the present study (including dilutions, cat. nos. and suppliers) is presented in Table I. After two washes with TBST, the membranes were incubated at room temperature for 1 h with HRP-conjugated secondary antibodies, including anti-rabbit IgG (HRP-linked; cat. no. 7074; Cell Signaling Technology, Inc.) and anti-mouse IgG (HRP-linked; cat. no. 7076; Cell Signaling Technology,

Inc.) antibodies, depending on the host species of the primary antibody, both diluted 1:4,000 in TBST containing 5% skim milk. Detection was performed using an ECL plus enhanced chemiluminescent substrate (GE Healthcare) and a ChemoDoc instrument (Bio-Rad Laboratories, Inc.). Densitometry was performed using Image Lab software (version 6.1.0; Bio-Rad Laboratories, Inc.). Equal loading was confirmed using actin staining.

Reverse transcription-quantitative PCR (RT-qPCR). Total RNA was extracted from TE cell lines or human PBMCs using the RNeasy Mini Kit (Qiagen GmbH) according to the manufacturer's protocol as previously described (22). cDNA was generated using 1 μ g RNA per reaction with Prime Script RT Master Mix (Takara Bio, Inc.) according to the manufacturer's protocol. RT-qPCR was performed using TaqMan Universal PCR Master Mix (No AmpErase UNG; Thermo Fisher Scientific, Inc.) and TaqMan probes (human CD40, Hs01002915_g1; human MMP-9, Hs00957562_m1; and human β -actin, Hs99999903_m1) on a Lightcycler instrument (Roche Diagnostics). The sequences of the primers and probes used in these assays are proprietary and not publicly disclosed by the manufacturer. The thermocycling conditions were as follows: Initial enzyme activation at 95°C for 10 min, followed by 40 cycles of denaturation at 95°C for 15 sec and annealing/extension at 60°C for 1 min. Data were analyzed using the $2^{-\Delta\Delta C_q}$ method (23), and β -actin was used as the reference gene for normalization.

CD40 mRNA expression was evaluated using semi-quantitative PCR. Total RNA was extracted from TE cells using the RNeasy Mini Kit (Qiagen GmbH) and quantified spectrophotometrically. Reverse transcription was performed using 1 μ g RNA with the Prime Script RT Master Mix (Takara Bio, Inc.) according to the manufacturer's protocol. The reverse transcription conditions were 37°C for 15 min and 85°C for 5 sec. The PCR reaction was performed with KOD Plus polymerase (Toyobo Co., Ltd.), which includes dNTPs in the reaction mixture, according to the manufacturer's instructions. The thermocycling conditions were as follows: 94°C for 2 min; 35 cycles of 98°C for 10 sec, 64°C for 1 sec and 68°C for 28 sec; followed by a hold at 10°C. The following primers were used: CD40 forward, 5'-AGAGTT CACTGAAACGGAATGCC-3' and reverse, 5'-ACAGGA TCCCGAAGATGATGG-3'; and β -actin forward, 5'-CAA CCGCGAGAAGATGACCC-3' and reverse, 5'-GGAACC GCTCATTGCCAATGG-3'. PCR products were separated on 2% agarose gels and visualized using ethidium bromide staining under UV light with a ChemoDoc instrument (Bio-Rad Laboratories, Inc.). Densitometric analysis was performed using Image Lab software (version 6.1.0; Bio-Rad Laboratories, Inc.). β -actin was used as the reference gene to confirm equal loading and for normalization.

The Prime PCR 96-well plate array ECM Remodeling H96 (cat. no. 10025275; Bio-Rad Laboratories, Inc.) was used according to the manufacturer's instructions to evaluate ECM-related gene expression. PCR was performed using the Lightcycler instrument (Roche Diagnostics) as aforementioned, and data were analyzed using the $\Delta\Delta C_q$ method. TE-5 and TE-10 EC cell lines were used in this assay.

Table I. Characteristics of the antibodies used in the present study.

Antigen	Cat. no.	Applications	Dilution	Manufacturer
CD40	ab13545	WB; ICC	1:1,000; 1:500	Abcam
	REA733	FC	1:50	Miltenyi Biotec GmbH
CD61	REA733	FC	1:50	Miltenyi Biotec GmbH
CD62P	REA389	FC	1:50	Miltenyi Biotec GmbH
CD154	REA238	FC	1:50	Miltenyi Biotec GmbH
β-actin	8H10D10	WB	1:1,000	Cell Signaling Technology, Inc.
p-Akt	4060T	WB	1:4,000	Cell Signaling Technology, Inc.
Akt	4691T	WB	1:4,000	Cell Signaling Technology, Inc.
p-p44/42 MAPK (Erk1/2)	4370T	WB	1:4,000	Cell Signaling Technology, Inc.
p44/42 MAPK (Erk1/2)	4695T	WB	1:4,000	Cell Signaling Technology, Inc.
p-JNK	4668T	WB	1:4,000	Cell Signaling Technology, Inc.
JNK	9252T	WB	1:4,000	Cell Signaling Technology, Inc.
NF-κB p65	8242T	WB	1:4,000	Cell Signaling Technology, Inc.
Histone H3	12648T	WB	1:4,000	Cell Signaling Technology, Inc.

FC, flow cytometry; ICC, immunocytochemistry; p-, phosphorylated; WB, western blotting.

Flow cytometry. The cells were first stained for the surface antigens CD40, CD154, CD61 and CD62P, followed by washing with autoMACS Rinsing Solution (Miltenyi Biotec GmbH). Cells were surface-stained for 10 min at 4°C with the following antibodies: CD40-VioBright™ FITC (cat. no. REA733; 1:50), CD154-allophycocyanin (cat. no. REA238; 1:50), CD61-VioBright™ 515 (cat. no. REA761; 1:50) and CD62P-phycoerythrin (cat. no. REA389; 1:500) (all from Miltenyi Biotec GmbH). Data were acquired using a MACSQuant® Analyzer 10 flow cytometer (Miltenyi Biotec GmbH) and analyzed using FlowJo software (version 10.6.2; Becton, Dickinson and Company).

Immunocytochemistry. Cells were cultured on coverslips and fixed with 3.7% formaldehyde for 15 min at 25°C. After three washes with PBS, the cells were blocked with PBS containing 3% BSA (Thermo Fisher Scientific, Inc.) and 10% (v/v) goat serum (Thermo Fisher Scientific, Inc.) for 15 min at 25°C. The cells were then incubated with human polyclonal anti-CD40 antibodies (1:500; cat. no. ab13545; Abcam) in PBS for 1 h at 25°C. After three PBS washes, the cells were incubated with Alexa Fluor® 488-conjugated goat anti-rabbit antibodies (1:500; cat. no. ab150077; Abcam) for 1 h at 25°C. After three PBS washes, the coverslips were mounted on slides using Dapi-Fluoromount-G™ (Southern Biotech), and the nuclei were labeled by staining with 4',6-diamidino-2-phenylindole. Permeabilization was not performed, as CD40 is a membrane protein with an extracellular epitope recognized by the antibody used. DAPI counterstaining was performed according to the manufacturer's instructions, which included incubation at room temperature for 5 min. Finally, the samples were analyzed using a confocal microscope (BZ-9000; Keyence Corporation) with the analysis software BZ-H3C (version 1.4.1; Keyence Corporation).

CD154 stimulation. Cells were treated with 5 μg/ml recombinant soluble CD154 (rsCD154; ENZO MEGACD40L;

Enzo Life Sciences) for 24 h in serum-free culture medium. After incubation at 37°C, the supernatants were harvested and centrifuged at 10,000 x g for 5 min at 4°C. Finally, the cell pellets were lysed using RNeasy kit (Qiagen GmbH), as described in the RT-qPCR section, for total RNA extraction. For the dose-response assay, TE-10 cells were treated under the same conditions with various concentrations of rsCD154 (10 ng/ml, 30 ng/ml, 100 ng/ml, 300 ng/ml, 1 μg/ml, 3 μg/ml, 10 μg/ml and 30 μg/ml) to evaluate MMP-9 mRNA expression in response to CD154 stimulation. The expression levels of MMP-9 mRNA were quantified using RT-qPCR as aforementioned.

Cell viability assay. The CellTiter 96 Aqueous One Solution Cell Proliferation Assay System (Promega Corporation) was used according to the manufacturer's instructions for the cell viability assays. Briefly, 4x10³ cells/well were plated into a 96-well plate and incubated for 48 h with or without stimulation with 5 μg/ml rsCD154 at 37°C in a humidified incubator with 5% CO₂. After 48 h of incubation, 10 μl CellTiter 96 Aqueous One Solution reagent was added to each well. The absorbance was measured at 490 nm using a SpectraMax I3 microplate reader (Molecular Devices, LLC) after 2 h of incubation at 37°C in a humidified 5% CO₂ atmosphere. A total of five replicate wells were used to measure cell viability.

Cell migration and invasion assays. Transwell cell migration assays were performed using 8-μm pore size membrane chambers without Matrigel (Corning BioCoat Control Inserts; cat. no. 354578; Corning, Inc.), while invasion assays were performed using Matrigel-coated chambers of the same type (Corning BioCoat Matrigel Invasion Chambers; cat. no. 354480; Corning, Inc.). A total of 5x10⁴ cells in 200 μl RPMI-1640 medium containing 1% FBS and 25 pg rsCD154 were seeded in the upper compartments, and 500 μl RPMI-1640 medium containing 10% FBS as a chemoattractant was added

to the lower compartments. After 48 h of incubation at 37°C in a humidified incubator with 5% CO₂, the non-invading cells were removed from the upper surface of the membrane by scrubbing with cotton-tipped swabs. Invasive cells on the membranes beneath the insert were fixed and stained using a Diff-Quick staining kit (Sysmex Corporation), which consists of a fixative solution, stain solution I and stain solution II. The membranes were sequentially immersed in each solution for 2 min at room temperature, according to the manufacturer's instructions. Stained cells were counted using a confocal microscope (BZ-9000; Keyence Corporation) and KEYENCE software (BZ H3C; version 1.4.1). A total of five fields were randomly selected, the total area of cells in each field was measured and the average was obtained to measure the number of invasive cells.

Gelatin zymography. Culture media from esophageal squamous cell carcinoma (ESCC) cells stimulated with or without 5 µg/ml rsCD154 for 24 h at 37°C were analyzed for gelatin degradation using 7.5% SDS-PAGE gels containing 0.1% (w/v) gelatin (from porcine skin type A; MilliporeSigma). After SDS-PAGE, the gels were washed twice for 1 h in 2.5% Triton X-100 and incubated for 24 h at 37°C in an incubation buffer [50 mM Tris (pH 7.4), 1 µM ZnCl₂, 5 mM CaCl₂ and 1% Triton X-100]. The gels were stained with 0.5% Coomassie brilliant blue R250 in methanol for 1 h at room temperature, and destained with a solution containing 40% methanol and 10% acetic acid for 4 h at room temperature. Gelatinolytic activity appeared as white bands on a blue background. The gels were scanned, and the protein band intensities were determined using a ChemiDoc image analyzer (Bio-Rad Laboratories, Inc.) and Image Lab software (version 6.1.0; Bio-Rad Laboratories, Inc.).

CD40 small interfering RNA (siRNA) transfection. CD40-specific and control siRNA were obtained from Santa Cruz Biotechnology, Inc. Control siRNA-A (cat. no. sc-37007) served as a non-targeting scrambled siRNA. CD40 siRNA (cat. no. sc-29250) was used to specifically knock down CD40 gene expression. The sequences of siRNAs were not provided by the supplier. TE-10 cells in the exponential growth phase were seeded into 96-well plates at a density of 7.5x10³ cells per well, cultured for 24 h, and then transfected with 800 nM siRNA using oligofectamine (Thermo Fisher Scientific, Inc.) and OPTI-MEM I reduced-serum medium (Thermo Fisher Scientific, Inc.) at 37°C for 4 h, according to the manufacturer's instructions. The siRNA concentration was determined based on prior dose-response experiments. After transfection, the cells were further incubated in complete growth medium at 37°C. Transfection efficiency was assessed 72 h post-transfection via flow cytometry using allophycocyanin-conjugated anti-CD40 antibodies for staining. Subsequent experiments were conducted 72 h after transfection. Control cells underwent mock transfection with control siRNA under identical conditions.

Signaling pathway assay. TE-10 cells (1x10⁵ cells/well) were seeded in 12-well plates, incubated at 37°C for 24 h and subsequently stimulated with 5 µg/ml rsCD154 for 15 or 30 min at room temperature. Cell pellets were collected at 15 and

30 min after stimulation. Proteins were then extracted from the cell pellets following the aforementioned western blotting protocol. The extracted proteins were analyzed using the antibodies listed in Table I to evaluate the activation of each signaling pathway involved in the CD40-CD154 interaction.

Platelet isolation. Venous blood was collected in an aplanic syringe containing 1/10 volume of CPD buffer (16 mM citric acid, 90 mM sodium citrate, 16 mM NaH₂PO₄, 142 mM dextrose, pH 7.4). Blood samples were centrifuged at 200 x g for 20 min at 20°C. The top layer containing platelet-rich plasma was transferred into a new tube containing 1 volume of HEP buffer (140 mM NaCl, 2.7 mM KCl, 3.8 mM HEPES, 5 mM EGTA, pH 7.4) and prostaglandin E₁ (1 µM final concentration; Cayman Chemical Company), and centrifuged at 100 x g for 20 min at 20°C. The supernatant was collected and placed into a new tube, which was centrifuged at 800 x g for 20 min at 20°C. After discarding the supernatant, the platelet pellet was washed twice with a platelet wash buffer [10 mM sodium citrate, 150 mM NaCl, 1 mM EDTA and 1% (w/v) dextrose, pH 7.4]. The platelet pellet was slowly resuspended in modified Tyrode buffer (134 mM NaCl, 12 mM NaHCO₃, 2.9 mM KCl, 0.34 mM Na₂HPO₄, 1 mM MgCl₂, 10 mM HEPES, 5 mM dextrose, 3 mg/ml BSA and 1 µM PGE₁, pH 7.4) and used as a platelet solution. Platelets were activated by pre-warming at 37°C for 5 min, followed by the addition of 1 U human α-thrombin (Prolytix). After thrombin addition, the mixture was allowed to stand at room temperature for 1 min.

ELISA. The concentrations of soluble CD154 (sCD154) and MMP-9 in the culture supernatant were measured using ELISA kits (Quantikine® ELISA: Human CD40 Ligand/TNFSF5 Immunoassay; cat. no. DCDL40; R&D Systems, Inc.; Quantikine® ELISA: Human MMP-9; cat. no. DMP900; R&D Systems, Inc.) according to the respective manufacturer's instructions. The optical density at 540 nm was determined using a SpectraMax I3 microplate reader (Molecular Devices, LLC). All samples were analyzed in quadruplicate.

Co-culturing TE cells and platelets. Briefly, 7.5x10⁴ TE-10 cells were inoculated into 24-well plates and incubated at 37°C for 24 h. After PBS washing, RPMI-1640 medium without FBS was added to the cells, and 1x10⁸ of the activated platelets suspended in 0.2 ml modified Tyrode solution were added to 0.4-µm-pore cell culture inserts and incubated at 37°C for another 24 h. After incubation, the culture supernatant and cell pellet were collected, and MMP-9 mRNA levels were determined using RT-qPCR as aforementioned. TaqMan probe-based assays were used (MMP-9: Hs00957562_m1; β-actin: Hs99999903_m1; Thermo Fisher Scientific, Inc.), and primer sequences were not disclosed by the supplier.

Analyzing MMP-9 and CD154 concentrations in the sera of patients undergoing EC surgery and determining their survival period. Approval was obtained from the Institutional Review Board of Hokkaido University Hospital (approval no. 24-0126; approval date July 10, 2024; Sapporo, Japan). Written informed consent was obtained from all patients who participated in this clinical research. The present study was conducted between August 2014 and October 2017 on 49 consecutive patients who

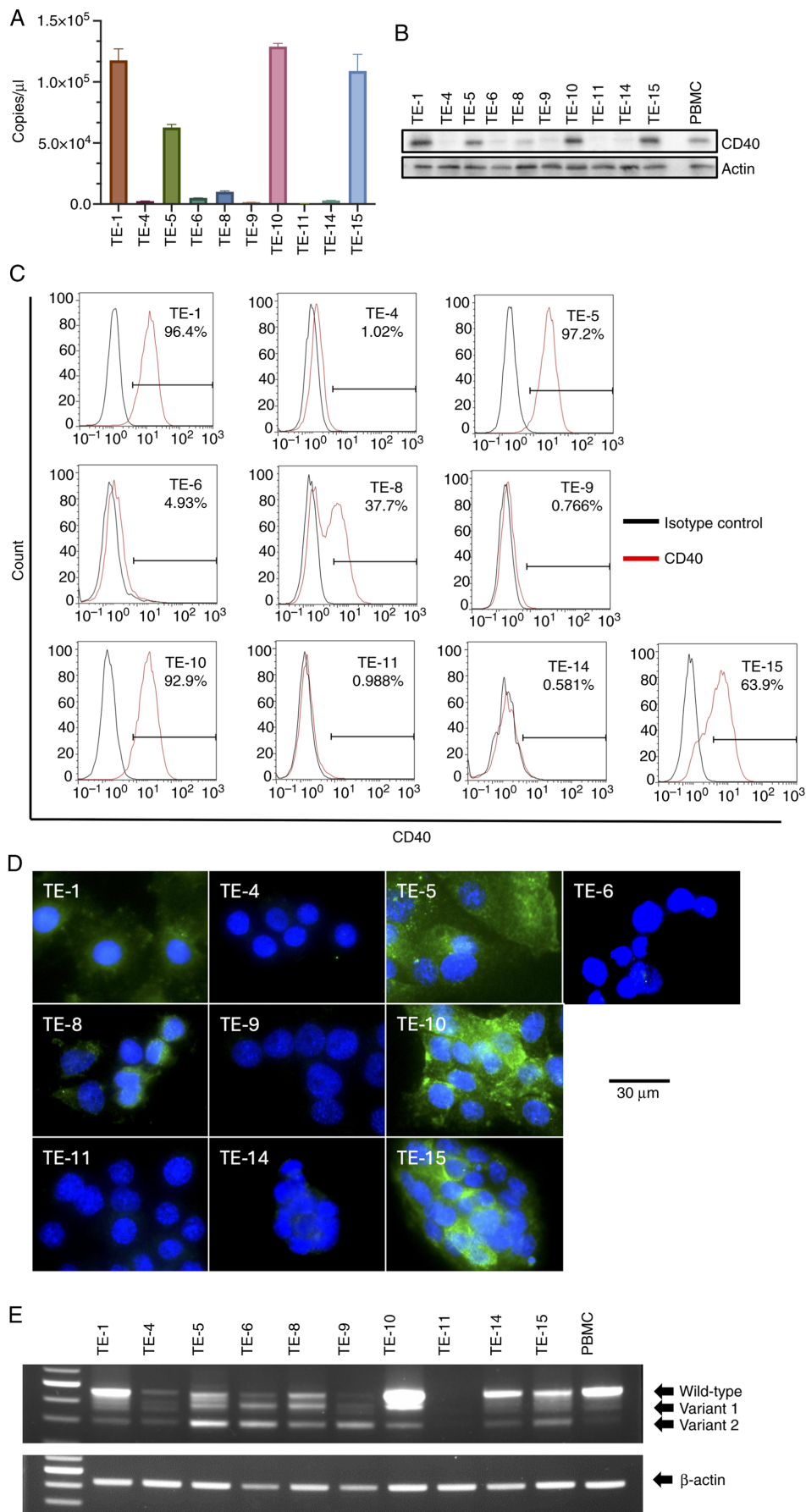


Figure 1. Analysis of CD40 expression in TE cells. (A) RT-qPCR. (B) Western blotting. (C) Flow cytometry. The percentage of CD40-positive cells is indicated in the figure. (D) Immunocytochemistry. CD40 was stained green and nuclei were stained blue. (E) Semi-RT-qPCR. The upper image shows the expression of CD40 mRNA splice variants, and the lower image shows β -actin expression as a reference gene for normalization. RT-qPCR, reverse transcription-quantitative PCR; PBMC, peripheral blood mononuclear cell.

underwent curative esophagectomy for EC at the Department of Gastroenterological Surgery, Hokkaido University Hospital (Sapporo, Japan). Eligible patients were aged ≥ 20 years and had provided informed consent to store blood samples for research purposes. Patients judged by the investigators to be inappropriate for inclusion were excluded. The survival analysis included 41 men and 8 women. The median age was 67 years, with an age range of 52-85 years. Patient sera were collected either immediately before surgery on the day of the operation or on the day prior to surgery, and stored at -80°C until further analyses. The samples were analyzed in August 2024. Serum MMP-9 and CD154 concentrations were measured using ELISA kits (Quantikine ELISA Human CD40 Ligand, Human MMP-9; R&D Systems, Inc.). Cancer recurrence and survival were analyzed over a minimum follow-up period of 5 years after esophagectomy. Information on cancer recurrence, survival time, TNM classification (Union for International Cancer Control 8th edition) (24) and histological type was extracted from the medical records.

Statistical analysis. All statistical analyses were performed using GraphPad Prism 9 software (Dotmatics). Pearson's χ^2 test, the unpaired t-test or the Mann-Whitney U test were used as appropriate to compare different groups. For comparisons involving three groups, one-way ANOVA was used, followed by Bonferroni post hoc analysis when statistical significance was detected. For survival analysis, the log-rank (Mantel-Cox) test was used to compare Kaplan-Meier survival curves. Data are presented as mean \pm SD, unless otherwise indicated. All experiments were performed in triplicate ($n=3$) unless stated otherwise. $P<0.05$ was considered to indicate a statistically significant difference.

Results

Analysis of CD40 expression on ESCC cells. CD40 mRNA expression was analyzed in 10 TE cell lines, among which TE-1, -5, -10 and -15 cells exhibited relatively high expression levels (Fig. 1A). Western blotting was performed to evaluate CD40 protein levels in TE cells. TE-1, -5, -10 and -15 cells showed clear CD40 bands (Fig. 1B). Flow cytometry and immunocytochemistry analyses were also performed to examine the cell surface expression of CD40 on TE cells, which revealed similar results to those obtained by western blotting, except for TE-1 cells, in which the immunocytochemistry result differed (Fig. 1C and D). No morphological differences were observed among the 10 types of TE cells based on CD40 expression, as assessed by Diff-Quick staining and light microscopy (Fig. S1). Due to discrepancies in CD40 expression levels across the different detection methods, such as weak or absent surface staining by immunocytochemistry in TE-1 cells despite positive results by RT-qPCR and western blotting, semi-quantitative PCR was also performed to further validate mRNA expression. Human CD40 is known to have splicing variants resulting from alternative splicing (25). The presence of splicing variants was confirmed in TE cells positive for CD40 mRNA expression (Fig. 1E). Based on these results, particular emphasis was placed on the flow cytometry and immunocytochemistry data. TE-5 and TE-10 cells, which exhibited high CD40 expression intensities, were selected as

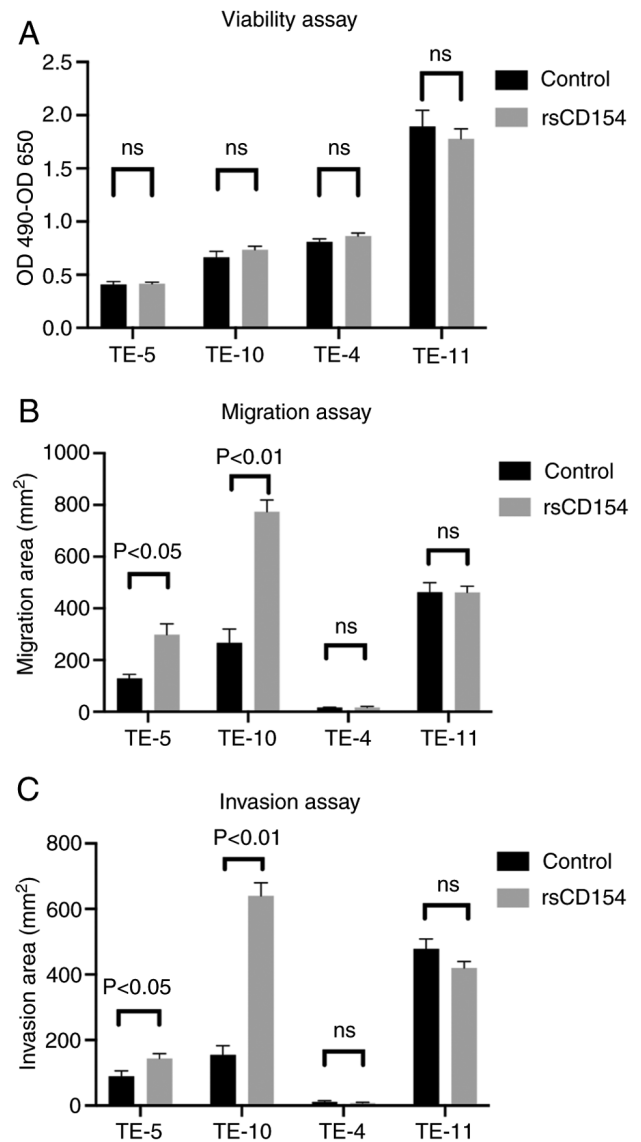


Figure 2. Functional analysis of cells stimulated with CD154. (A) Viability assay. No significant changes were observed in all four cell lines. (B) Migration assay. (C) Invasion assay. Migration and invasion were enhanced in TE-5 and TE-10 cells, which highly expressed CD40, after rsCD154 stimulation. No significant changes were observed in low CD40 expression cells (TE-4 and -11 cells). The Mann-Whitney U test was performed using GraphPad Prism 9 software. ns, not significant; OD, optical density; rsCD154, recombinant soluble CD154.

CD40-overexpressing cells for subsequent experiments, while TE-4 and TE-11 cells, which had low CD40 expression intensities, were used as low CD40 expression cells.

CD154 stimulation assay of TE cells. CD40 activation was performed *in vitro* to assess changes in TE cell activity and investigate the function of CD40 in EC. In the present study, CD154, a CD40 ligand, was used to activate CD40. The four types of TE cells showed no morphological differences (Fig. S1); however, their baseline viability, migration and invasion varied. Notably, TE-11 cells exhibited high viability and invasion (Figs. 2 and S2). TE cells did not exhibit significant changes in proliferative ability, regardless of the presence or absence of CD40 expression (Fig. 2A). No changes in cell migration or invasion were observed in low CD40 expression

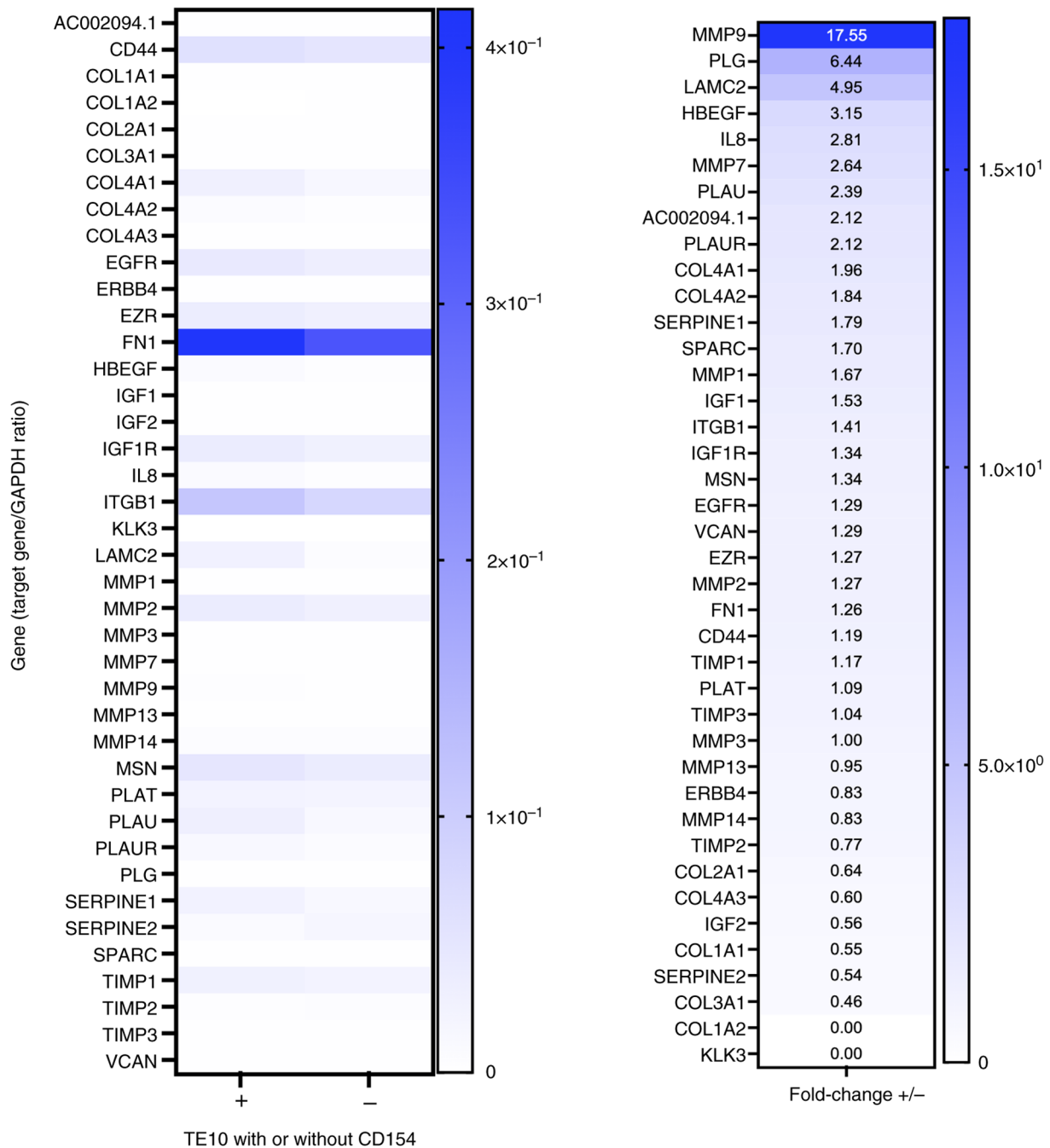


Figure 3. Changes in gene expression caused by the CD40-CD154 interaction in TE-10 cells. Screening of 40 genes involved in extracellular matrix remodeling. The expression ratios of target genes relative to GAPDH are shown on the left. On the right, CD154-induced changes in gene expression are displayed in descending order. Upregulation of gene expression in the order MMP-9 > PLG > LAMC2 was confirmed following rsCD154 stimulation.

cells upon stimulation with rsCD154. By contrast, high CD40 expression cells exhibited significantly increased migration and invasion (Figs. 2B and C, and S2). Although baseline differences in viability, migration and invasion were observed among the cell lines investigated in the present study, the results suggested that the CD40-CD154 interaction in TE cells enhanced cell motility without changing their proliferative capacity. These interactions were only observed in high CD40 expression cells.

Changes in gene expression levels upon CD40-CD154 interaction. Changes in gene expression levels in TE-10 cells due to the

CD40-CD154 interaction were examined. The genes involved in ECM remodeling were investigated because no change in cell viability was observed, whereas cell migration and invasion were increased. The expression levels of 40 genes related to changes in ECM remodeling were screened. Specifically, following stimulation with rsCD154, the mRNA expression level of MMP-9 increased by 17.55-fold, that of plasminogen (PLG) by 6.44-fold, and that of laminin subunit γ -2 (LAMC2) by 4.95-fold in TE-10 cells (Fig. 3). The analysis was also performed in TE-5 cells, where a similarly strong upregulation of MMP-9 mRNA was observed (Fig. S3). Therefore, MMP-9 expression was investigated in subsequent experiments.

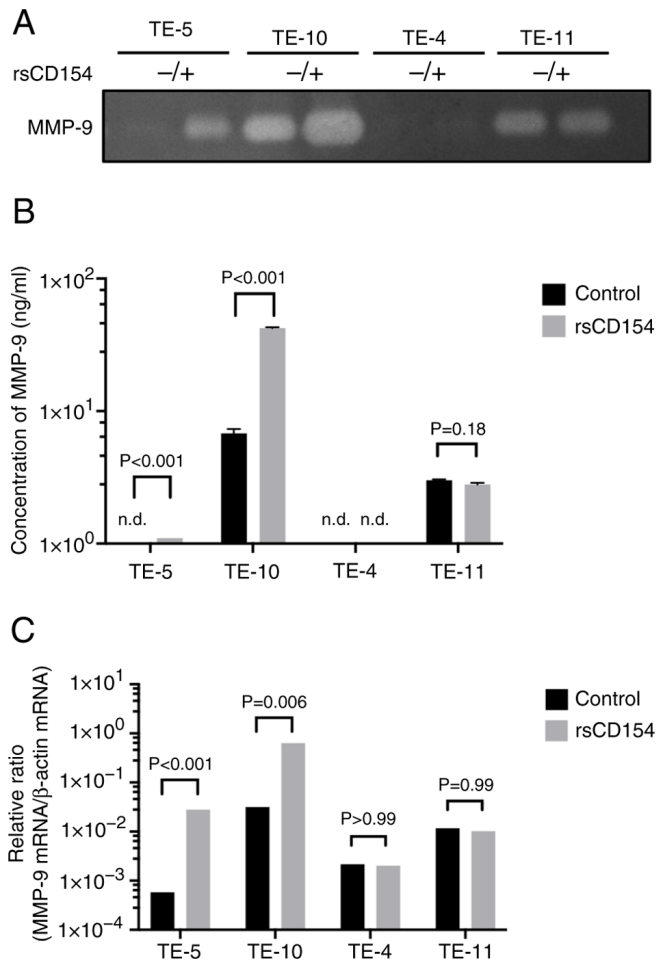


Figure 4. Changes in MMP-9 expression caused by the CD40-CD154 interaction in TE cells. (A) Qualitative analysis of MMP-9 secretion from TE cells using gelatin zymography. Increased MMP-9 secretion was observed in high CD40 expression cells (TE-5 and -10), regardless of the baseline MMP-9 secretion level without CD154 stimulation. (B) Quantitative analysis of MMP-9 secretion from TE cells using an ELISA. Increased MMP-9 secretion was observed in TE-5 and -10 cells. (C) Quantitative analysis of MMP-9 mRNA expression in TE cells via reverse transcription-quantitative PCR. MMP-9 mRNA expression upregulation was observed in high CD40 expression cells (TE-5 and -10). The Mann-Whitney U test was performed using GraphPad Prism 9 software. n.d., not detected; rsCD154, recombinant soluble CD154.

It was determined whether the CD40-CD154 interaction induced MMP-9 secretion. rsCD154 and PBS (control) were added to TE cells, and MMP-9 secretion in the culture supernatant was analyzed via gelatin zymography (Fig. 4A) and ELISA (Fig. 4B). MMP-9 upregulation was observed in the culture supernatants of high CD40 expression cells, whereas MMP-9 expression in low CD40 expression cells did not change significantly. TE-10 and TE-11 cells, which exhibited higher baseline invasive abilities in migration and invasion assays, also exhibited elevated MMP-9 levels even without sCD154 stimulation. Next, MMP-9 regulation was assessed at the mRNA level. After rsCD154 stimulation, MMP-9 mRNA expression was upregulated in high CD40 expression TE cells, whereas no change was observed in low CD40 expression cells (Fig. 4C). Additionally, the upregulation of MMP-9 mRNA induced by CD154 stimulation occurred in a dose-dependent manner (Fig. S4).

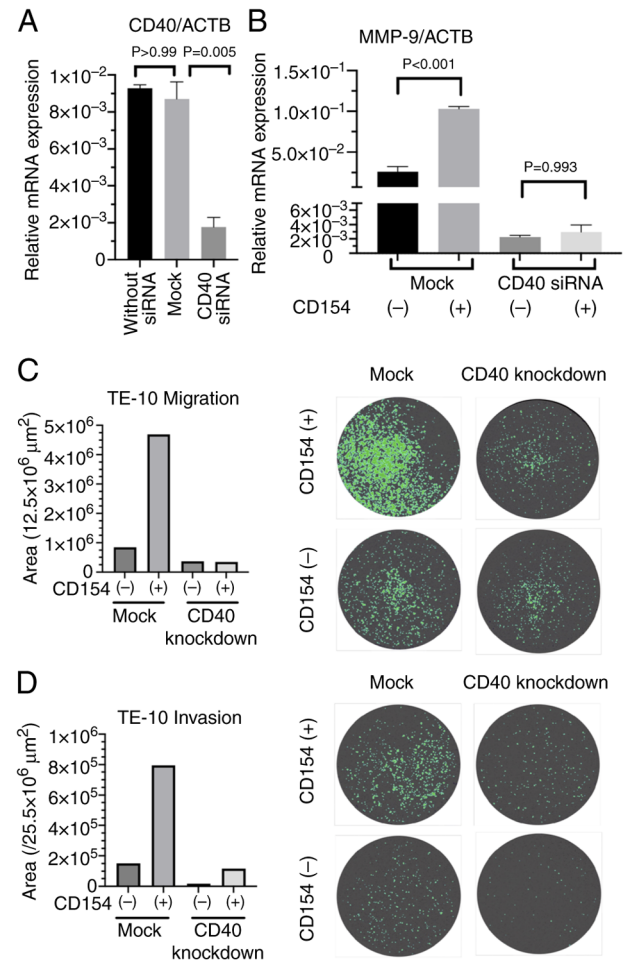


Figure 5. Experiments using CD40-knockdown TE-10 cells using siRNA. (A) Transfection with CD40 siRNA resulted in a reduction in CD40 mRNA expression. The average relative CD40 mRNA expression was compared using GraphPad Prism 9 software. After one-way ANOVA, Bonferroni post hoc analysis was performed. (B) CD154 stimulation of CD40 knockdown TE-10 cells was performed, and MMP-9 upregulation was suppressed. (C) Migration assay. CD40 knockdown reduced cell migration, and no increase in migration was observed following CD154 stimulation. The images on the right present a visualization of migrating cells under a 1.25x optical microscope, with the cellular regions indicated by green labelling. (D) Invasion assay. Similar to the migration assay, a decrease in invasion was observed following CD40 knockdown. The images on the right present a visualization of migrating cells under a 1.25x optical microscope, with the cellular regions indicated by green labelling. siRNA, small interfering RNA.

Changes in TE-10 cell function induced by CD40 knockdown. To elucidate the role of the CD40 gene in TE cells, CD40-knockdown TE-10 cells were generated. Transfection of TE-10 cells with si-CD40 or si-control resulted in the creation of CD40 knockdown TE-10 cells and control TE-10 cells (Mock), respectively. The knockdown efficiency was then evaluated by measuring CD40 mRNA levels using qPCR (Fig. 5A). Additionally, the response of these cells to sCD154 stimulation was assessed by measuring MMP-9 mRNA levels. CD40-knockdown TE-10 cells consistently exhibited low MMP-9 mRNA levels regardless of sCD154 stimulation (Fig. 5B). Furthermore, migration and invasion assays were performed using CD40-knockdown TE-10 cells. The results demonstrated that CD40-knockdown TE-10 cells exhibited reduced migratory and invasive capabilities compared with the control cells (Fig. 5C and D).

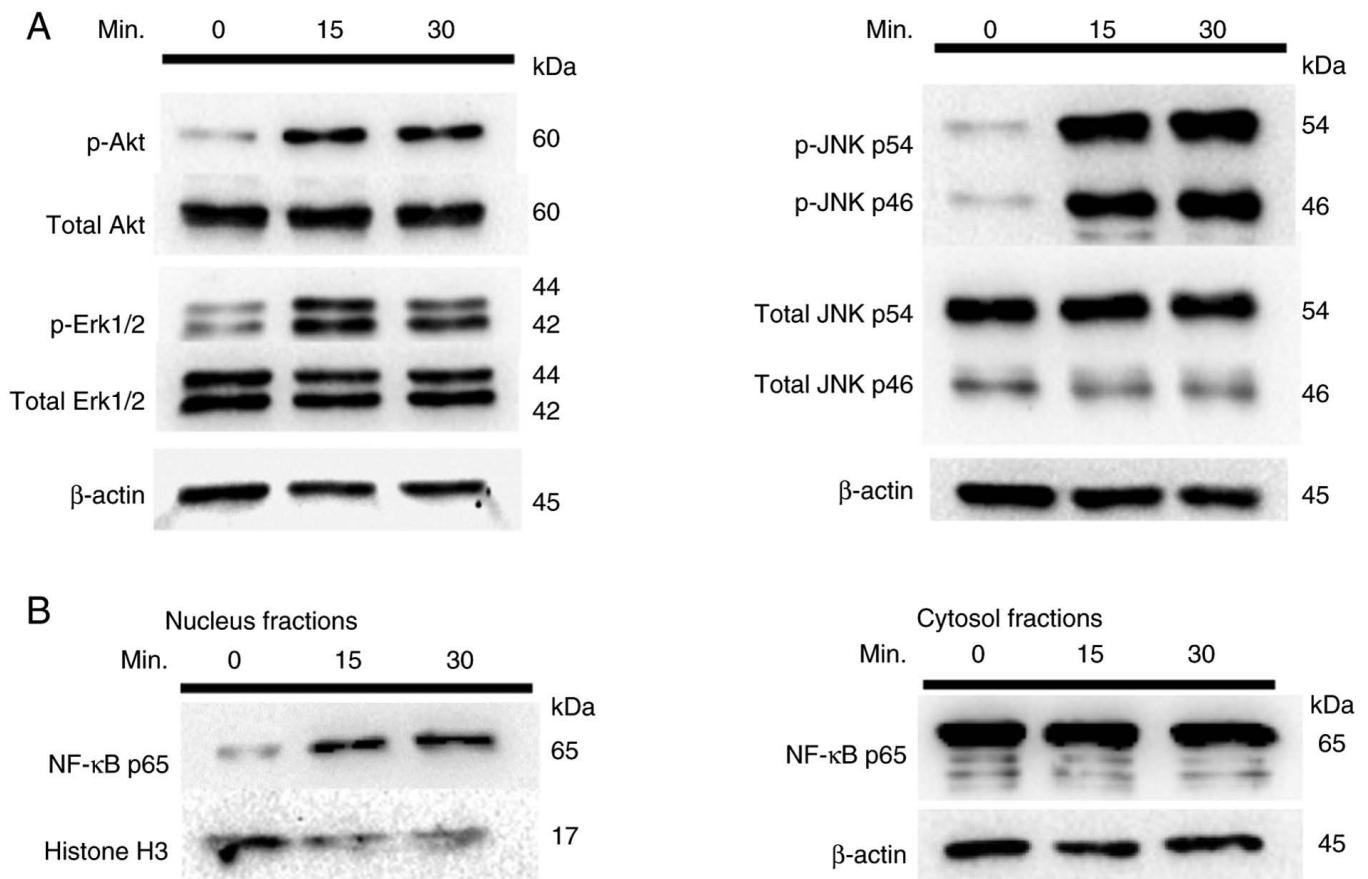


Figure 6. Signaling pathway assay. (A) CD40 activation induced phosphorylation of Akt, Erk1/2 and JNK, indicating the activation of the PI3K/Akt and MAPK pathways. (B) Phosphorylation of NF-κB was observed in the nuclear fraction, indicating activation of the NF-κB pathway. Cells were stimulated with rsCD154, and samples were collected for western blot analysis using phosphorylation-specific antibodies. p-, phosphorylated.

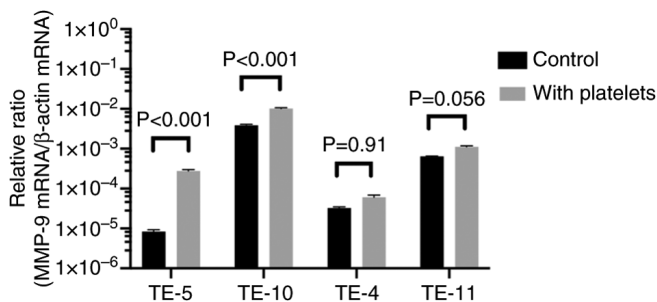


Figure 7. Changes in MMP-9 mRNA levels following co-culture of TE cells with activated platelets. MMP-9 mRNA expression upregulation was observed in TE-5 and -10 cells co-cultured with the platelet solution. The Mann-Whitney U test were performed using GraphPad Prism 9 software.

CD40 signaling pathway in TE-10 cells. Given that the CD40-CD154 interaction induces MMP-9 upregulation, the activation of PI3K, MAPK and NF-κB was investigated following CD40 activation in TE-10 cells. As shown in Fig. 6A, phosphorylation of Akt, a downstream effector of PI3K, was observed in CD154-stimulated TE-10 cells, confirming PI3K activation. Furthermore, phosphorylation of Erk1/2 and JNK, indicating MAPK pathway activation, is also shown in Fig. 6A. Nuclear translocation of NF-κB p65 was also observed, as shown in Fig. 6B, indicating its activation.

Platelet extraction and MMP-9 upregulation in TE cells induced by CD154-expressing human platelets. *In vivo*, CD154 exists either as a transmembrane protein on the surface of CD4⁺ T lymphocytes or as a soluble form. The majority of circulating sCD154 is derived from platelets (26), which are activated by proteinaceous platelet-activating factors secreted by cancer cells in the tumor microenvironment (TME). The viability and metastasis of cancer cells are promoted by the induction of platelet aggregation (26-28). Therefore, the relationship between platelets and high CD40 expression EC cells was evaluated. Platelet solutions were prepared using blood samples collected from healthy human donors. Because platelets are activated in the TME and engage tumor cells (29), α-thrombin was used to activate platelets in the present study.

The purity of the generated platelet solution was confirmed via flow cytometry for platelet marker CD61 expression (30). Platelets were activated via α-thrombin stimulation, and their activity was confirmed by detecting CD62P (P-selectin) expression, an activated platelet marker (Fig. S5). Thrombin-activated platelets exhibited a slight increase in CD154 expression on their cell surface (Fig. S6). In addition, sCD154 release into the platelet solution was increased (Fig. S7). Next, four types of TE cells were co-cultured with the platelet solution to observe the reaction between the platelet solution and EC cells. MMP-9 mRNA upregulation was confirmed in all four types of TE cells; however, the increase was statistically significant only in

Table II. Patient characteristics (n=49).

Characteristics	Value
Median age, years (interquartile range)	67 (63-74)
Sex, n (%)	
Male	41 (83.7)
Female	8 (16.3)
Histopathological type, n (%)	
Squamous cell carcinoma	46 (93.9)
Adenocarcinoma	3 (6.1)
Pathological T stage, UICC 8th, n (%)	
T1	31 (63.3)
T2	2 (4.1)
T3	14 (28.6)
T4	2 (4.1)
Pathological N stage, UICC 8th, n (%)	
N0	30 (61.2)
N1	8 (16.3)
N2	7 (14.3)
N3	4 (8.2)
Pathological M stage, UICC 8th, n (%)	
M0	49 (100)
Pathological stage, UICC 8th, n (%)	
IA	8 (16.3)
IB	16 (32.7)
IIA	1 (2.0)
IIB	8 (16.3)
IIIA	1 (2.0)
IIIB	11 (22.4)
IVA	4 (8.2)
Platelet count, $\times 10^3/\mu\text{l}$ (mean \pm SD)	227.5 \pm 65.0
Serum MMP-9 level, ng/ml (mean \pm SD)	534.1 \pm 384.3
Serum CD154 level, ng/ml (mean \pm SD)	2.2 \pm 1.1
3-year overall survival, %	66.3
3-year disease-free survival, %	58.5

UICC, Union for International Cancer Control.

TE-5 and TE-10 cells, which exhibited high CD40 expression (Fig. 7).

Survival analysis of patients undergoing esophagectomy. Esophagectomies were performed on 49 patients during the study period. The median age of the patients was 67 years, and 41 patients were male. The 3-year overall survival (OS) rate was 66.3%, and the 3-year disease-free survival (DFS) rate was 58.5% (Table II). The MMP-9 concentration was 534.1 \pm 384.3 ng/ml (mean \pm SD), and the CD154 concentration was 2.15 \pm 1.12 ng/ml (mean \pm SD). In the univariate analysis, platelet counts were significantly higher in the high MMP-9 group, and a trend toward elevated platelet counts was observed in the high CD154 group (Tables SI and SII). The relationship between the survival period and the concentrations of MMP-9 and CD154 was evaluated using Kaplan-Meier curves, with patients stratified into high and low expression groups

based on the median value. No significant association was observed between serum MMP-9 or CD154 levels and OS or DFS (Fig. 8A-D). However, when survival was analyzed based on serum MMP-9 and serum CD154 levels stratified by pathological stage (pStage I and II-IV), a significant improvement in prognosis was noted for patients with low MMP-9 levels in pStage I (Fig. 9A and C). By contrast, low MMP-9 levels were significantly associated with reduced OS in patients with pStage II-IV (Fig. 9G). Serum CD154 levels did not exhibit any association with survival, even when analyzed according to pStage.

Discussion

In the present study, several notable findings were reported. First, it was demonstrated that the CD40-CD154 interaction promoted MMP-9 secretion in EC cells, increasing their invasiveness (Fig. 10). Second, the involvement of platelets in enhancing CD40-mediated MMP-9 secretion in EC cells was revealed. Third, the preliminary analysis of sera from patients undergoing esophagectomy indicated a possible association between MMP-9 levels and survival time.

CD40 is expressed on APCs and serves a crucial role as a co-stimulatory molecule in immune responses, including anti-tumor immunity. However, CD40 is also expressed in cancer cells, where its activation increases IL-8, IL-10, IL-12p40 and tumor growth factor- β secretion, contributing to apoptosis evasion, cell viability and immune escape (14,31). The present study also demonstrated that the upregulation of ECM remodeling molecules such as MMP-9, PLG and LAMC2 via the MAPK, NF- κ B and PI3K/Akt pathways contributes to cancer invasion and metastasis. These findings suggested that the CD40-CD154 interaction in cancer cells may create a favorable environment for cancer cell viability. CD40 expression in cancer cells is a poor prognostic factor; however, this may not be true for all cancer types. For example, CD40 ligand stimulation did not alter viability in cell lines co-expressing CD40 and CD154, whereas stimulation with CD40- and CD154-blocking antibodies decreased cell viability and reduced immunoregulatory cytokine secretion (IL-6, IL-10 and IL-12p40) (14). These findings suggest that autocrine CD40 activity is enhanced in cell lines co-expressing CD40 and CD154, contributing to increased cancer cell invasion.

CD40 expression in the TME affects tumor invasion, metastasis and antitumor immunity (5). The balance between cancer cell invasion and immunity changes depending on CD154 secretion from host platelets, CD154 expression by the cancer cells themselves and the response of the surrounding lymphocytes (3,4). Based on these findings, a hypothesis was proposed to further explore the dynamics of CD40-CD154 interactions in the TME. Specifically, these interactions were categorized into four conceptual patterns, according to the presence or absence of CD40 and CD154 expression in tumor cells, as discussed subsequently.

Based on the aforementioned observations, we hypothesized the following regarding the potential roles of CD40-CD154 interactions in the TME: When both CD40 and CD154 are expressed, CD40-CD154 interactions are enhanced through autocrine signaling among cancer cells, T lymphocytes and platelets, promoting tumor progression.

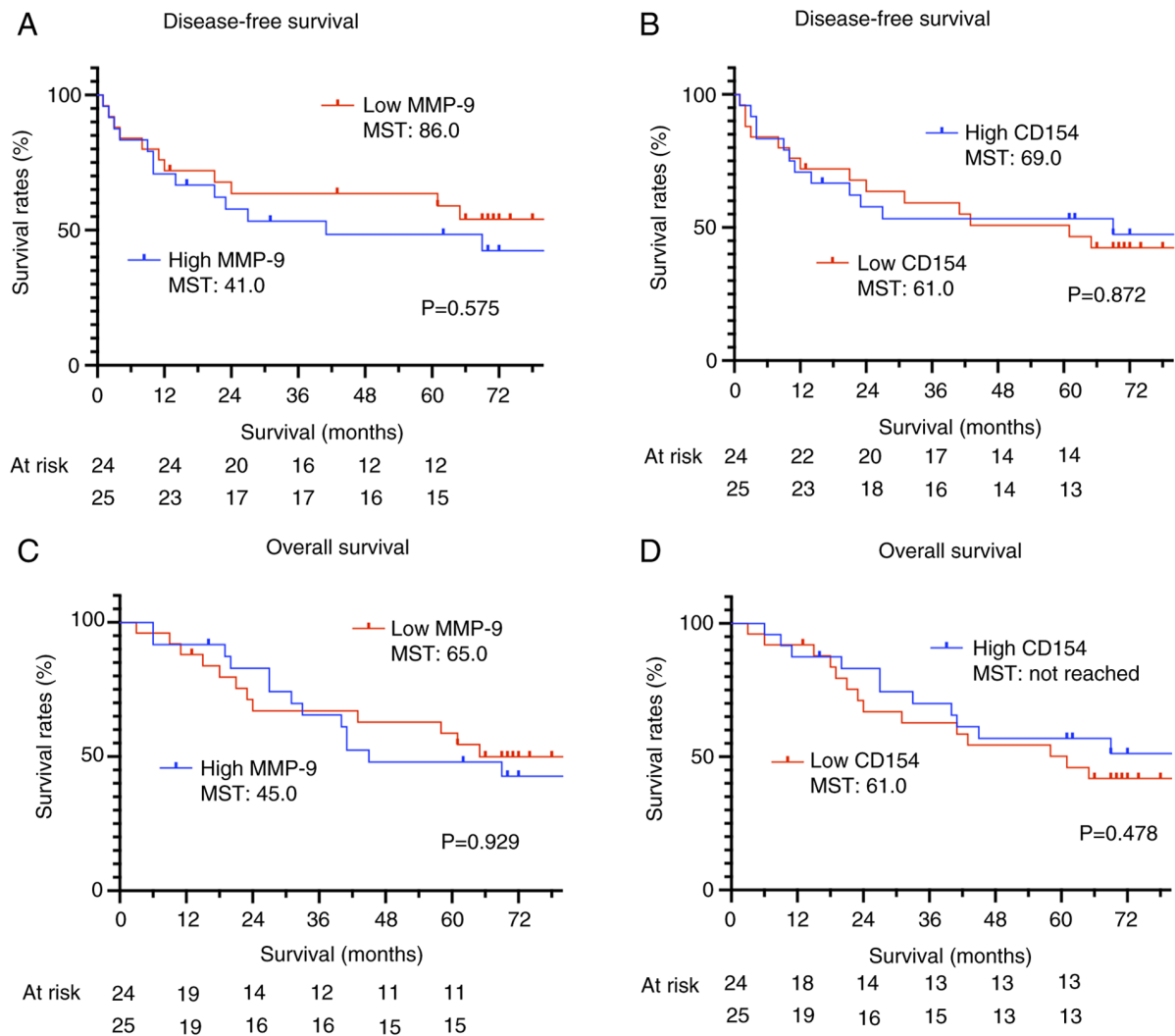


Figure 8. Survival analysis of patients who underwent esophagectomy was performed using the Kaplan-Meier method. The log-rank (Mantel-Cox) test was conducted using GraphPad Prism 9 software. (A) Association between DFS and MMP-9 levels. (B) Association between DFS and CD154 levels. (C) Association between OS and MMP-9 levels. (D) Association between OS and CD154 levels. DFS, disease-free survival; MST, median survival time; OS, overall survival.

Concurrently, cancer cell-derived CD154 stimulates CD40 on APCs, enhancing tumor immunity. Therefore, whether tumor progression or antitumor immunity becomes dominant is determined by the relative strength of CD40-CD154-mediated cancer cell invasion vs. immune activation. For example, CD40 and CD154 co-expression is a poor prognostic factor in melanoma (9) and renal cancer (32), indicating a tendency towards malignancy. Second, in cases where only CD40 is expressed, CD40-CD154 interactions are enhanced by CD154 from T lymphocytes or platelets, promoting tumor progression without affecting tumor immunity. Consequently, cancer cell viability is predominant. Third, CD40-CD154 interactions do not affect tumor progression when only CD154 is expressed, resulting in stable tumor progression. However, CD40 expression in APCs is stimulated by cancer cell-derived CD154, enhancing tumor immunity and resulting in a dominant antitumor immune response. In cervical cancer, CD154 positivity is associated with improved survival (33). Lastly, when neither CD40 nor CD154 is expressed, CD40-CD154 interactions do not affect tumor progression or immunity.

Survival analysis using serum samples from patients with EC who underwent surgery revealed intriguing results. While no significant association was observed between serum MMP-9 or serum CD154 levels and survival across all patients, stage-specific survival analysis showed a significant association between serum MMP-9 levels and survival. In patients with stage I EC, high MMP-9 levels were associated with poor prognosis, whereas in patients with stage II-IV EC, low MMP-9 levels were associated with poor overall survival, but not with disease-free survival. In patients with EC eligible for surgery (that is, those without distant metastases), MMP-9 levels could reflect the metastatic potential of a tumor. Conversely, in patients with established metastases, tumor progression at metastatic sites might decrease MMP-9 levels. In the present study, the stage I high MMP-9 group and the stage II-IV high MMP-9 group exhibited comparable prognoses. Specifically, the 5-year OS rate was 38.5% in the stage I high MMP-9 group and 54.5% in the stage II-IV high MMP-9 group. The 5-year DFS rates were also similar, at 38.5 and 45.5%, respectively. Despite the difference in staging, these groups may share similar biology in terms of metastasis and invasion. The opposite

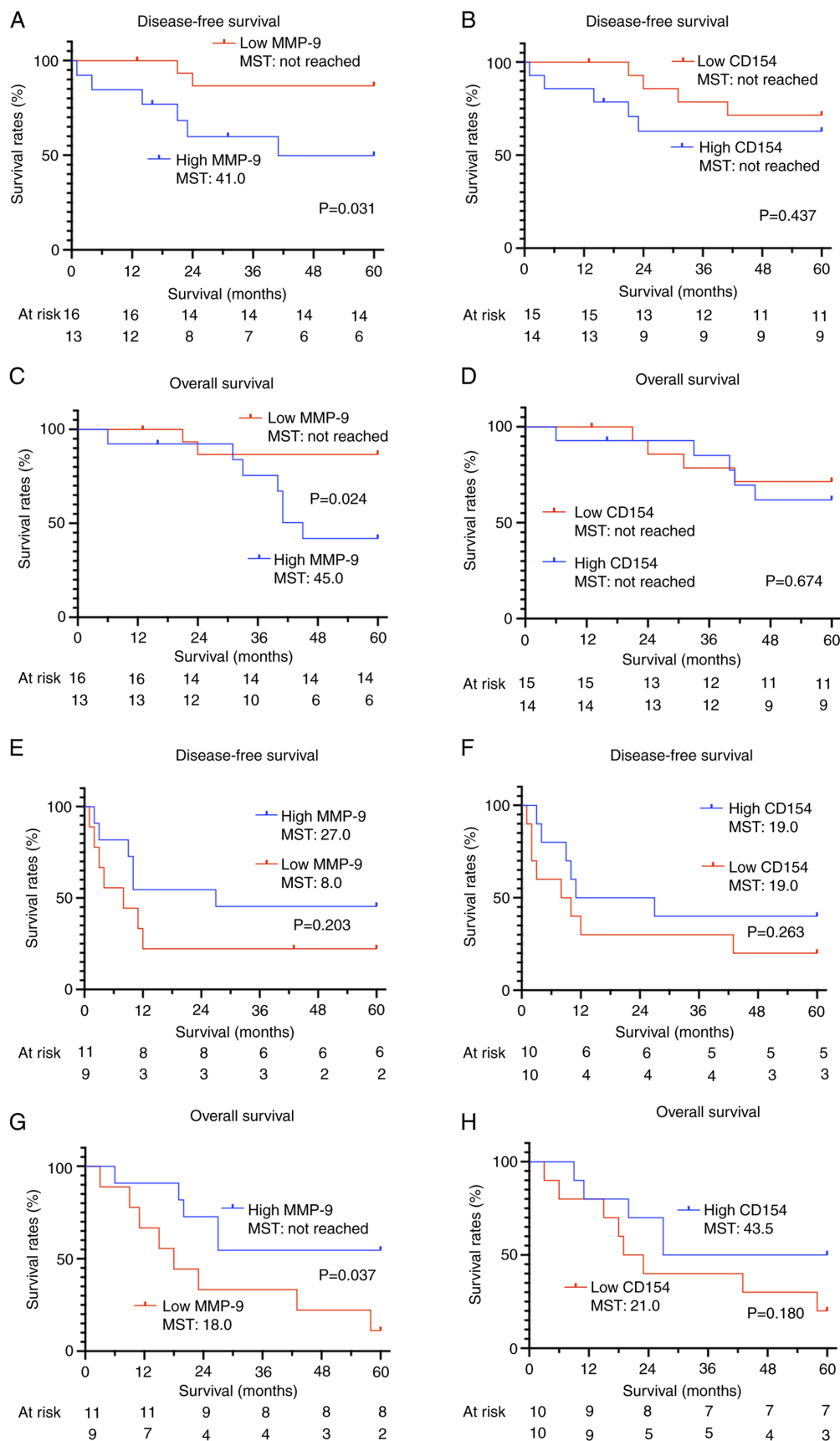


Figure 9. Survival analysis of patients with esophageal cancer stratified by disease stage. (A) Association between DFS and MMP-9 levels in patients with pathological stage I. (B) Association between DFS and CD154 levels in patients with pathological stage I. (C) Association between OS and MMP-9 levels in patients with pathological stage I. (D) Association between OS and CD154 levels in patients with pathological stage I. (E) Association between DFS and MMP-9 levels in patients with pathological stage II-IV. (F) Association between DFS and CD154 levels in patients with pathological stage II-IV. (G) Association between OS and MMP-9 levels in patients with pathological stage II-IV. (H) Association between OS and CD154 levels in patients with pathological stage II-IV. Survival analysis was performed using the Kaplan-Meier method, and the log-rank (Mantel-Cox) test was conducted using GraphPad Prism 9 software. DFS, disease-free survival; MST, median survival time; OS, overall survival.

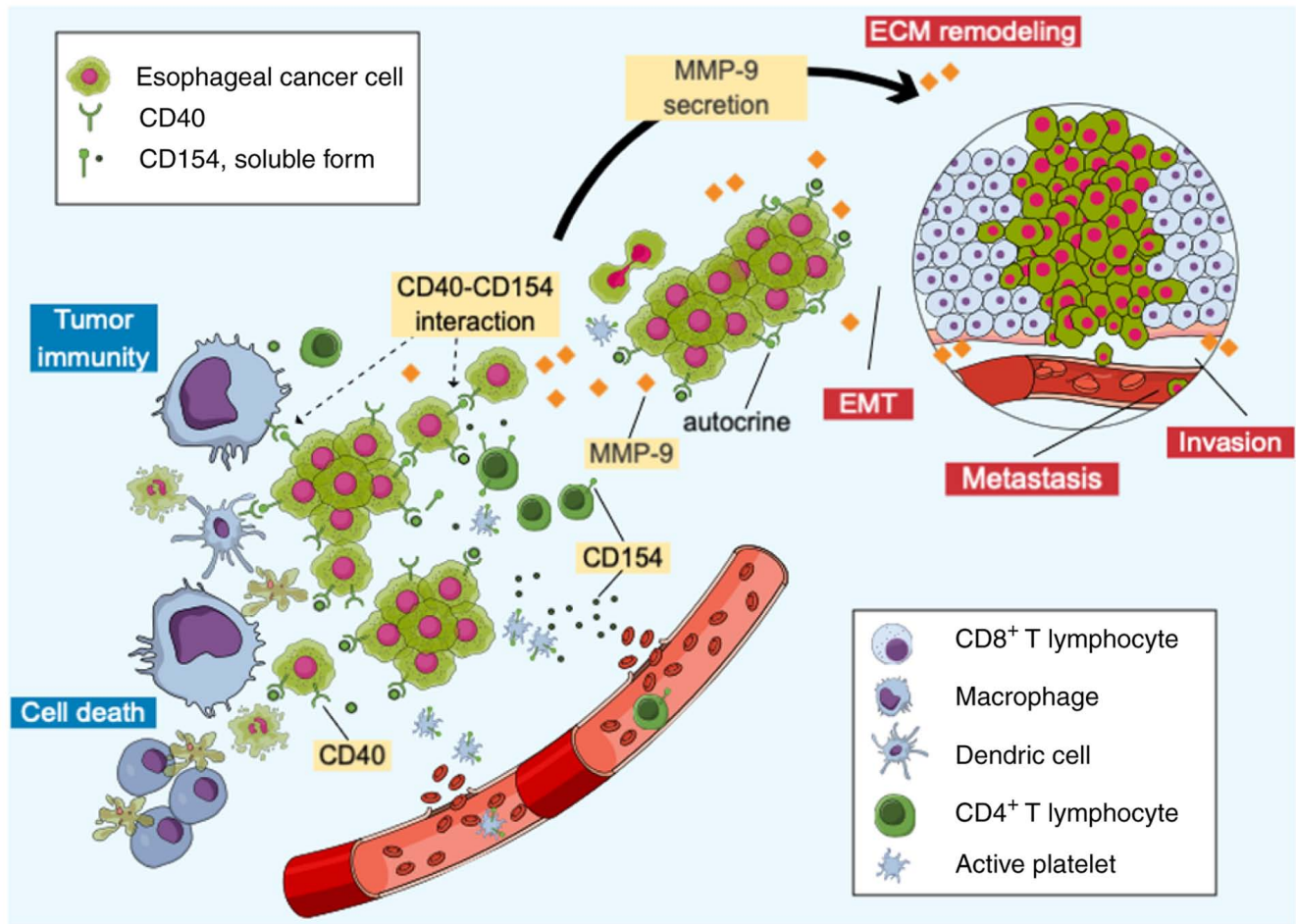


Figure 10. Schema of the CD40-CD154 interaction in the tumor microenvironment of esophageal cancer. In tumor cells, the CD40-CD154 interaction induces the secretion of molecules involved in ECM remodeling, including MMP-9, contributing to cell invasion, EMT and metastasis. In immune cells, the CD40-CD154 interaction is involved in antitumor immunity, leading to cancer cell death. ECM, extracellular matrix; EMT, epithelial-mesenchymal transition.

association observed between MMP-9 levels and survival in early- vs. advanced-stage disease may reflect stage-specific differences in the underlying metastatic processes (34). While further studies are needed to confirm these observations, MMP-9 levels may have potential as a prognostic biomarker when interpreted in the context of disease stage.

The results of the present study were verified at the cellular level; however, experiments using cell lines limited to *in vitro* conditions may not consistently reproduce the *in vivo* TME. Furthermore, the survival analysis has limitations as it is a retrospective study conducted at a single institution with a small number of cases.

In conclusion, the present *in vitro* experiments demonstrated that CD40 expression in EC cells enhanced migration and invasion upon CD154 stimulation, accompanied by increased MMP-9 secretion, suggesting a potential role in promoting tumor aggressiveness.

Acknowledgements

Not applicable.

Funding

No funding was received.

Availability of data and materials

The data generated in the present study may be requested from the corresponding author.

Authors' contributions

KU designed and conducted the experiments, and drafted the manuscript. TN contributed to the study design, critically revised the manuscript for important intellectual content and provided expert advice throughout the project. KS contributed to conducting the experiments and compiling the data. OS and TS assisted with the experimental procedures. SH contributed to the study design, provided critical revisions of the manuscript and supervised the scientific direction of the project. KU and TN confirm the authenticity of all the raw data. All authors have read and approved the final version of the manuscript.

Ethics approval and consent to participate

Approval (approval no. 24-0126; approval date July 10, 2024) was obtained from the Institutional Review Board of Hokkaido University Hospital (Sapporo, Japan). Written informed consent was obtained from all patients participating in the present study.

Patient consent for publication

Not applicable.

Competing interests

The authors declare that they have no competing interests.

References

- Torre LA, Bray F, Siegel RL, Ferlay J, Lortet-Tieulent J and Jemal A: Global cancer statistics, 2012. *CA Cancer J Clin* 65: 87-108, 2015.
- Pennathur A, Gibson MK, Jobe BA and Luketich JD: Oesophageal carcinoma. *Lancet* 381: 400-412, 2013.
- van Kooten C and Banchereau J: CD40-CD40 ligand. *J Leukoc Biol* 67: 2-17, 2000.
- Schonbeck U and Libby P: The CD40/CD154 receptor/ligand dyad. *Cell Mol Life Sci* 58: 4-43, 2001.
- Richards DM, Sefrin JP, Gieffers C, Hill O and Merz C: Concepts for agonistic targeting of CD40 in immuno-oncology. *Hum Vaccin Immunother* 16: 377-387, 2020.
- Xu W, Li Y, Yuan WW, Yin Y, Song WW, Wang Y, Huang QQ, Zhao WH and Wu JQ: Membrane-bound CD40L promotes senescence and initiates senescence-associated secretory phenotype via NF- κ B activation in lung adenocarcinoma. *Cell Physiol Biochem* 48: 1793-1803, 2018.
- Lim CY, Chang JH, Lee WS, Kim J and Park IY: CD40 agonists alter the pancreatic cancer microenvironment by shifting the macrophage phenotype toward M1 and suppress human pancreatic cancer in organotypic slice cultures. *Gut and Liver* 16: 645-659, 2022.
- Bishop GA, Moore CR, Xie P, Stunz LL and Kraus ZJ: TRAF proteins in CD40 signaling. *Adv Exp Med Biol* 597: 131-151, 2007.
- van den Oord JJ, Maes A, Stas M, Nuyts J, Battocchio S, Kasran A, Garmyn M, De Wever I and De Wolf-Peters C: CD40 is a prognostic marker in primary cutaneous malignant melanoma. *Am J Pathol* 149: 1953-1961, 1996.
- Sabel MS, Yamada M, Kawaguchi Y, Chen FA, Takita H and Bankert RB: CD40 expression on human lung cancer correlates with metastatic spread. *Cancer Immunol Immunother* 49: 101-108, 2000.
- Li R, Chen WC, Pang XQ, Hua C, Li L and Zhang XG: Expression of CD40 and CD40L in gastric cancer tissue and its clinical significance. *Int J Mol Sci* 10: 3900-3917, 2009.
- Ishikawa K, Miyamoto M, Yoshioka T, Kato T, Kaji M, Ohbuchi T, Hirano S, Itoh T, Dosaka-Akita H and Kondo S: Up-regulation of CD40 with juxtacrine activity in human nonsmall lung cancer cells correlates with poor prognosis. *Cancer* 113: 530-541, 2008.
- Cooke PW, James ND, Ganesan R, Wallace M, Burton A and Young LS: CD40 expression in bladder cancer. *J Pathol* 188: 38-43, 1999.
- Shoji Y, Miyamoto M, Ishikawa K, Yoshioka T, Mishra R, Ichinokawa K, Matsumura Y, Itoh T, Shinohara T, Hirano S and Kondo S: The CD40-CD154 interaction would correlate with proliferation and immune escape in pancreatic ductal adenocarcinoma. *J Surg Oncol* 103: 230-238, 2011.
- Matsumura Y, Hiraoka K, Ishikawa K, Shoji Y, Noji T, Hontani K, Itoh T, Nakamura T, Tsuchikawa T, Shichinohe T and Hirano S: CD40 expression in human esophageal squamous cell carcinoma is associated with tumor progression and lymph node metastasis. *Anticancer Res* 36: 4467-4475, 2016.
- Davidson B, Reich R, Risberg B and Nesland JM: The biological role and regulation of matrix metalloproteinases (MMP) in cancer. *Arch Patol* 64: 47-53, 2002.
- Rhee JS and Coussens LM: RECKing MMP function: Implications for cancer development. *Trends Cell Biol* 12: 209-211, 2002.
- Egeblad M and Werb Z: New functions for the matrix metalloproteinases in cancer progression. *Nat Rev Cancer* 2: 161-174, 2002.
- Dagouassat M, Suffee N, Hlawaty H, Haddad O, Charni F, Laguillier C, Vassy R, Martin L, Schischmanoff PO, Gattegno L, *et al*: Monocyte chemoattractant protein-1 (MCP-1)/CCL2 secreted by hepatic myofibroblasts promotes migration and invasion of human hepatoma cells. *Int J Cancer* 126: 1095-1108, 2010.
- Nakamura T, Kuwai T, Kim JS, Fan D, Kim SJ and Fidler IJ: Stromal metalloproteinase-9 is essential to angiogenesis and progressive growth of orthotopic human pancreatic cancer in parabiont nude mice. *Neoplasia* 9: 979-986, 2007.
- Rigothier C, Daculsi R, Lepreux S, Auguste P, Villeneuve J, Dewitte A, Doudnikoff E, Saleem M, Bourget C, Combe C and Ripoche J: CD154 induces matrix metalloproteinase-9 secretion in human podocytes. *J Cell Biochem* 117: 2737-2747, 2016.
- Takeuchi S, Baghdadi M, Tsuchikawa T, Wada H, Nakamura T, Abe H, Nakanishi S, Usui Y, Higuchi K, Takahashi M, *et al*: Chemotherapy-derived inflammatory responses accelerate the formation of immunosuppressive myeloid cells in the tissue microenvironment of human pancreatic cancer. *Cancer Res* 75: 2629-2640, 2015.
- Livak KJ and Schmittgen TD: Analysis of relative gene expression data using real-time quantitative PCR and the 2(-Delta Delta C (T)) method. *Methods* 25: 402-408, 2001.
- Brierley JD, Gospodarowicz MK, Wittekind C, editors. *BNBrierley JD, Gospodarowicz MK, Wittekind C, editors. TNM Classification of Malignant Tumours*. 8th ed. Oxford: Wiley-Blackwell; 2017.
- Tone M, Tone Y, Fairchild PJ, Wykes M and Waldmann H: Regulation of CD40 function by its isoforms generated through alternative splicing. *Proc Natl Acad Sci USA* 98: 1751-1756, 2001.
- Schlesinger M: Role of platelets and platelet receptors in cancer metastasis. *J Hematol Oncol* 11: 125, 2018.
- Haemmerle M, Stone RL, Menter DG, Afshar-Kharghan V and Sood AK: The platelet lifeline to cancer: Challenges and opportunities. *Cancer Cell* 33: 965-983, 2018.
- Gay LJ and Feldin-Habermann B: Contribution of platelets to tumour metastasis. *Nat Rev Cancer* 11: 123-134, 2011.
- Goubran H, Sabry W, Kotb R, Seghatchian J and Burnouf T: Platelet microparticles and cancer: An intimate cross-talk. *Transfus Apher Sci* 53: 168-172, 2015.
- Blair TA and Frelinger AL 3rd: Platelet surface marker analysis by mass cytometry. *Platelets* 31: 633-640, 2020.
- Chatzigeorgiou A, Lyberi M, Chatzilymperis G, Nezos A and Kamper E: CD40/CD40L signaling and its implication in health and disease. *Biofactors* 35: 474-483, 2009.
- Bussolati B, Russo S, Deambrosio I, Cantaluppi V, Volpe A, Ferrando U and Camussi G: Expression of CD154 on renal cell carcinomas and effect on cell proliferation, motility and platelet-activating factor synthesis. *Int J Cancer* 100: 654-661, 2002.
- Grazia GA, Bastos DR and Villa LL: CD40/CD40L expression and its prognostic value in cervical cancer. *Braz J Med Biol Res* 56: e13047, 2023.
- Pantel K and Brakenhoff RH: Dissecting the metastatic cascade. *Nat Rev Cancer* 4: 448-456, 2004.



Copyright © 2025 Umemoto et al. This work is licensed under a Creative Commons Attribution-NonCommercial-NoDerivatives 4.0 International (CC BY-NC-ND 4.0) License.